Toward Resolving the Outflow Engine: An Observational Perspective

Tom Ray

Dublin Institute for Advanced Studies

Catherine Dougados

Laboratoire d'Astrophysique de Grenoble

Francesca Bacciotti

INAF-Osservatorio Astrofisico di Arcetri

Jochen Eislöffel

Thüringer Landessternwarte Tautenburg

Antonio Chrysostomou

University of Hertfordshire

Jets from young stars represent one of the most striking signposts of star formation. The phenomenon has been researched for over two decades and there is now general agreement that such jets are generated as a by-product of accretion; most likely by the accretion disk itself. Thus they mimic what occurs in more exotic objects such as active galactic nuclei and micro-quasars. The precise mechanism for their production however remains a mystery. To a large degree, progress is hampered observationally by the embedded nature of many jet sources as well as a lack of spatial resolution: Crude estimates, as well as more sophisticated models, nevertheless suggest that jets are accelerated and focused on scales of a few AU at most.

It is only in the past few years however that we have begun to probe such scales in detail using classical T Tauri stars as touchstones. Application of adaptive optics, data provided by the HST, use of specialised techniques such as spectro-astrometry, and the development of spectral diagnostic tools, are beginning to reveal conditions in the jet launch zone. This has helped enormously to constrain models. Further improvements in the quality of the observational data are expected when the new generation of interferometers come on-line. Here we review some of the most dramatic findings in this area since Protostars and Planets IV including indications for jet rotation, i.e. that they transport angular momentum. We will also show how measurements, such as those of width and the velocity field close to the source, suggest jets are initially launched as warm magneto-centrifugal disk winds.

Finally the power of the spectro-astrometric technique, as a probe of the central engine in very low mass stars and brown dwarfs, is shown by revealing the presence of a collimated outflow from a brown dwarf for the first time, copying what occurs on a larger scale in T Tauri stars.

1. INTRODUCTION

The phenomenon of jets from young stellar objects (YSOs) has been known for over two decades. While we now have a reasonably good understanding of how they propagate and interact with their surroundings on large scales (e.g., see the chapter by *Bally, Reipurth and Davis*), i.e. hundreds of AU and beyond, how precisely these jets are generated remains a puzzle. The observed correlation between mass outflow and accretion through the star's disk (e.g. *Hartigan et al.*, 1995; *Cabrit et al.*, 1990) would seem to favour some sort of magnetohydrodynamic (MHD) jet launching mechanism but which one is open to question.

In particular it is not known whether jets originate from the interface between the star's magnetosphere and disk (the so-called X-wind model, see the chapter by *Shang et al.*; *Shang et al.*, 2002; *Shu et al.*, 2000) or from a wide range of disk radii (the disk or D-wind model, see the chapter by *Pudritz et al.*).

On the observational front we have begun to probe the region where the jet is generated and collimated, thus testing the various models. Moreover since Protostars and Planets IV a number of major advances have been made thanks to the availability of high angular resolution imaging and spectroscopy. In particular the use of intermediate dis-
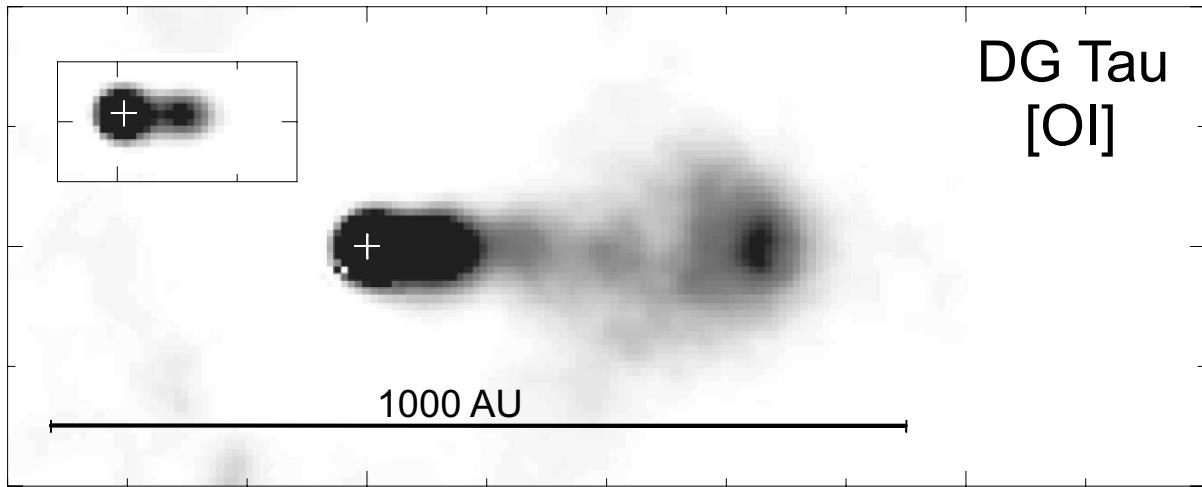
Fig. 1.— Deconvolved [OI]λ6300 + continuum narrow-band image of the DG Tau jet obtained with the AO system PUEO on the Canada-France-Hawaii Telescope. The spatial resolution achieved was $0''1 = 14$ AU at the distance of the Taurus Auriga Cloud. Inset (top-left) is a high contrast image near the source. Adapted from *Dougados et al.,* (2002).

person spectroscopy (long-slit, Fabry-Perot or employing integral field units) has provided excellent contrast between the line emitting outflow and its continuum-generating parent YSO, a pre-requisite to trace outflows right back to their source (see Section 2). Examples include ground-based telescopes equipped with Adaptive Optics (AO) and the Space Telescope Imaging Spectrograph (STIS), giving angular resolution down to $0''05$ (see Section 2 & Section 3). In addition, as will be explained below, the technique of spectro-astrometry (see Section 5) is providing insights on scales of a few AU from the source. The new methodologies have brought an impressive wealth of morphological and kinematical data on the jet-launching region (≤ 200 AU from the YSO) providing the most stringent constraints to date for the various models. Here we will illustrate these results, e.g. measurements of the jet diameter close to the source, and, where appropriate, comparison with model predictions.

Jets may be Nature's way of removing excess angular momentum from accretion disks, thereby allowing accretion to occur. Moreover, they are produced not only by young stars but by a plethora of astronomical objects from nascent brown dwarfs, with masses of around $5.10^{-2}M_\odot$, to black holes at the centre of AGN, as massive as $5.10^8 M_\odot$. In between they are generated by X-ray binaries, symbiotic systems, planetary nebulae, and gamma ray burst sources (e.g., *Livio*, 2004). The range of environments, and the astounding 10 orders of magnitude in mass over which the jet mechanism operates, is testimony to its robustness. Thus understanding how they are generated is of wide interest to the Astrophysics Community. Given the quality of data now coming on stream, and the prospect of even better angular resolution in the near future, we are hopefully close to unravelling the nature of the engine itself. Our suspicion, as supported below, is that this will be done first in the context of YSO outflows.

2. IMAGING STRUCTURES CLOSE TO THE JET BASE

YSO jets largely emit in a number of atomic and molecular lines (see, for example, *Reipurth and Bally*, 2001 or *Eislöffel et al.*, 2000). In the infrared to the ultra-violet, these lines originate in the radiative cooling zones of shocks with typical velocities from a few tens to a few hundred km s^{-1}. Thus in order to explore the morphology and kinematics of the jet launching zone, both high spatial resolution narrow-band imaging (on sub-arcsecond scales) and intermediate resolution spectroscopy is required. Leaving aside interferometry of their meagre radio continuum emission (*Girart et al.*, 2002), currently the best spatial resolution is afforded by optical/NIR instruments. Many YSOs are so deeply embedded however that optical/NIR observations are impossible. That said, one class of evolved YSO, namely the classical T Tauri stars (CTTS), are optically visible and have jets (see Fig. 1). CTTS therefore offer a unique opportunity to test current ejection theories. In particular, they give access to the innermost regions of the wind (≤ 100 AU) where models predict that most of the collimation and acceleration processes occur. Moreover the separate stellar and accretion disk properties of these systems are well known. Here we summarise what has been learned from recent high-angular resolution imaging studies of a number of CTTS jets. These observations have been conducted either from the ground with adaptive optics (AO) or from space with the Hubble Space Telescope (HST).

A fundamental difficulty in imaging a faint jet close to a bright CTTS is contrast with the source itself. This problem is often further exacerbated by the presence of an extended reflection nebula. Contrast with the line emitting jet can be improved either by decreasing the PSF (with AO systems from the ground or by imaging from space with, e.g., HST) and by increasing the spectral resolution.
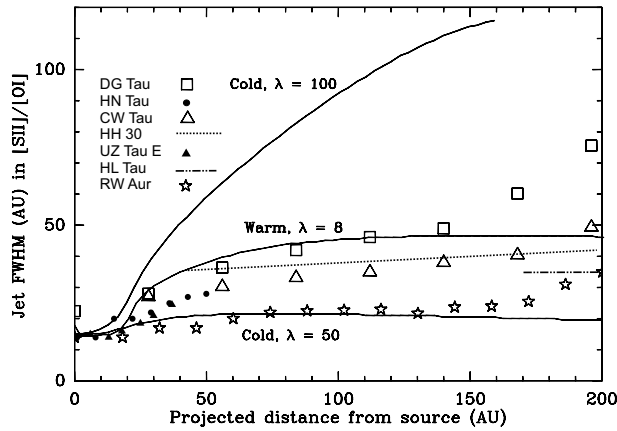
2

Fig. 2.— Variation of jet width (FWHM) derived from [SII] and [OI] images as a function of distance from the source. Data points are from CFHT/PUEO and HST/STIS observations made by the authors as well as those of *Hartigan et al.,* (2004). Overlaid (solid lines) are predicted variations based on two cold disk wind models with low efficiency (high λ) and a warm disk solution for comparison from *Dougados et al.,* (2004). Note that moderate to high efficiency is favoured, i.e. warm solutions. Here efficiency is measured in terms of the ratio of mass outflow to mass accretion. Models are convolved with a 14 AU (FWHM) gaussian beam. For full details see *Garcia et al.,* (2001) and *Dougados et al.,* (2004).

Obviously the optimum solution is a combination of both. The pioneering work of *Hirth et al.,* (1997) used long-slit spectroscopy with accurate central continuum subtraction to reveal spatial extensions of a few arcseconds in the forbidden line emission of a dozen CTTS. Around the same time, narrow-band imaging with the HST provided the first high spatial resolution images of jets from CTTS (*Ray et al.*, 1996). More recently application of AO systems from the ground on 4m-class telescopes, using both conventional narrow-band imaging and in combination with intermediate spectral resolution systems, have led to remarkable 0″2 resolution images of a number of small-scale jets from CTTS including DG Tau, CW Tau, and RW Aur (*Dougados et al.*, 2000; *Lavalley et al.*, 1997; *Lavalley-Fouquet et al.*, 2000). An alternative approach, pioneered by *Hartigan et al.,* (2004), is "slit-less spectroscopy″ using high spatial resolution instruments such as the STIS on board the HST. The advantage of this method is that, providing the dispersion of the spectrograph is large enough, one can obtain non-overlapping emission-line images covering a large range of wavelengths. This includes lines where no narrow-band HST filters exist. In this way *Hartigan et al.,* (2004) constructed high spatial resolution images of the jets from CW Tau, HN Tau, UZ Tau E, DF Tau, and the primary of DD Tau. Moreover, as will be described fully in the next section, the use of contiguous parallel long-slits, for example with STIS, can also provide high resolution "images" not only in individual lines but over a range of velocities

(see Section 3 and, for example, *Woitas et al.*, 2002).

All of these observations show that these "small-scale″ T Tauri jets have complex morphologies, dominated by emission knots, that strongly resemble the striking HH jets emanating from IRAS Class 0/1 sources (see the chapter by *Bally, Reipurth, and Davis*). Turning to larger scales, deep ground-based imaging by *Mundt and Eislöffel,* (2000) revealed that CTTS jets are associated with faint bow-shock like structures, at distances of a few thousand AU. Moreover *McGroarty and Ray*, (2004) found that CTTS outflows can stretch for several parsecs as is the case with outflows from more embedded YSOs. Thus the observations clearly suggest that the same ejection mechanism is at work at all phases of star formation.

Images taken at different epochs, usually a few years apart, can reveal how the outflow varies with time. For example, large proper motions, on the order of the jet flow velocity, have been inferred for the knots in the DG Tau and RW Aur jets (*Dougados et al.*, 2000; *López-Martín et al.*, 2003; *Hartigan et al.*, 2004). In the DG Tau jet, a clear bow-shaped morphology is revealed for the knot located at 3″ (*Lavalley et al.*, 1997; *Dougados et al.*, 2000) as well as jet wiggling, suggestive of precession. These properties, as in the younger HH flows, suggest that knots are likely to be internal working surfaces due to time variable ejection. Detailed hydrodynamical modelling, for example of the DG Tau jet, indicate fluctuations on time scales of 1-10 yrs, although one single period does not seem to account for both the kinematics and the morphology (*Raga et al.*, 2001). Such rapid changes are also observed at the base of the younger, embedded HH flows. Attempts at modelling these changes have been made. For example, numerical simulations by *Goodson et al.,* (1999) of the interaction of the stellar magnetosphere with the disk predict a cyclic inflation of the former leading to eruptive ejection. The estimated timescales, however, seem too short as they are around a few stellar rotation periods. It is also possible that such short term fluctuations in the outflow may come from disk instabilities or cyclic changes in the stellar magnetic field (as in the Sun). Further study is clearly needed to give insight into the origin of the variability process.

Imaging studies close to the YSO reveal details that are useful in discriminating between various models. For example plots of jet width (FWHM) against distance from the source, are shown in Fig 2 for a number of CTTS outflows (HL Tau, HH 30: *Ray et al.*, 1996; DG Tau, CW Tau, and RW Aur: *Dougados et al.*, 2000, *Woitas et al.*, 2002). Similar results were found by *Hartigan et al.*, (2004) for the jets from HN Tau and UZ Tau E (see Fig 2). These studies show that at the highest spatial resolution currently achieved (0″1 = 14 AU for the Taurus Auriga Star Formation Region), the jet is unresolved within 15 AU from the central source. Moreover large opening angles (20-30 degrees) are inferred for the HN Tau and UZ Tau E jets on scales of 15-50 AU, indicating widths at the jet source <5 AU (*Hartigan et al.*, 2004). Beyond 50 AU, HH jets seem to slowly increase in width with much smaller opening angles of a few degrees.

FWHM of 20-40 AU are inferred at projected distances of around 100 AU from the central source. Such measurements demonstrate that collimation is achieved on scales of a few tens of AU, i.e. close to the YSO, and appear to rule out pure hydrodynamic models for their focusing (see, for example, *Frank and Mellema*, 1996).

Here we note that synthetic predictions of jet widths, taking into account projection and beam dilution effects, have been computed for self-similar disk wind solutions (e.g., *Ferreira*, 1997 and *Casse and Ferreira*, 2000). The variation of jet diameter with distance from the source is consistent with disk wind models of moderate to high efficiency ($\dot{M}_{eject}/\dot{M}_{acc} > 0.03$) (e.g., *Garcia et al.*, 2001, *Dougados et al.*, 2004 and Fig 2). Here efficiency is defined as the ratio of the total bipolar jet mass flux to the accretion rate.

3. KINEMATICS: VELOCITY PROFILES, ROTATION, ACCELERATION AND IMPLICATIONS

Spectra of CTTS with jets frequently reveal the presence of two or more velocity components (*Hartigan et al.*, 1995). In long-slit spectra with the slit oriented along the jet direction, the so-called high-velocity component (HVC), with velocities as large as a few hundred $km\,s^{-1}$, appears more extended and of higher excitation than the low-velocity component (LVC), which has velocities in the range 10–50 $km\,s^{-1}$ (*Hirth et al.*, 1997; *Pyo et al.*, 2003).

In order to understand the nature of such components, the region of the jet base (first few hundred AU) has to be observed with sufficient spectral resolution. This can be done using integral field spectroscopy, ideally employing AO, to produce 3-D data cubes (2-D spatial, 1-D radial velocity). Slices of the data-cubes then give 2-D images of a jet at different velocity intervals, akin to the 'channel maps' of radio interferometry. For example *Lavalley-Fouquet et al.,* (2000) used OASIS to map the kinematics of the DG Tau jet with 0.″5 resolution (corresponding to 70 AU at the distance of DG Tau). Even better spatial resolution, however, can be achieved with HST although a long-slit, rather than an integral field spectrograph has to be employed (*Bacciotti et al.*, 2000; *Woitas et al.*, 2002). In particular the jets from RW Aur and DG Tau were studied with multiple exposures of a 0.″1 slit, stepping the slit transversely across the outflow every 0.″07. Combining the exposures together, in different velocity bins, again provided channel maps (see Fig. 3). In such images, the jets show at their base an onion-like kinematic structure, being more collimated at higher velocities and excitation. The high velocity 'spine' can be identified with the HVC. The images also show, however, progressively wider, slower and less excited layers further from the outflow axis, in a continuous transition between the HVC and the LVC. At a distance of about 50-80 AU from the source, though, the low-velocity material gradually disappears, while the axial HVC is seen to larger distances. The flow as a whole thus *appears* to accelerate on scales of 50-100 AU. This structure has recently been shown to extend to the external H_2-emitting portion

of the flow (*Takami et al.*, 2004). All of these properties have been predicted by theoretical models of magneto-centrifugal winds (see, for example, the chapters by *Shang et al.* and *Pudritz et al.*).

The most exciting finding in recent years, however, has been the detection of radial velocity asymmetries that could be interpreted as *rotation* of YSO jets around their axes. Early hints of rotation were found in the HH 212 jet at large distance ($\approx 10^4$ AU) from the source by *Davis et al.,* (2000). More recently indications for rotation have been obtained in the first 100 - 200 AU of the jet channel through high angular resolution observations, both from space and the ground (*Bacciotti et al.*, 2002; *Coffey et al.*, 2004; *Woitas et al.*, 2005). Such velocity asymmetries have been seen in all the T Tauri jets observed with HST/STIS (DG Tau, RW Aur, CW Tau, Th 28, and HH 30), in different emission lines and using slit orientations both parallel and perpendicular to the outflow axis. For example at optical wavelengths, systematic shifts in radial velocity, typically from 5 to 25 ± 5 $km\,s^{-1}$, were found at jet positions displaced symmetrically with respect to the outflow axis, at 50 - 60 AU from the source and 20 - 30 AU from the axis (see Fig. 4). Note that the resolving power of STIS in the optical is around 55 $km\,s^{-1}$. Applying, however, gaussian fitting and cross-correlation routines to the line profiles, it is possible to detect velocity shifts as small as 5 $km\,s^{-1}$. It should also be mentioned that the sense and degree of velocity asymmetry suggesting rotation were found to be consistent in different elements of various systems (e.g., both lobes of the bipolar RW Aur jet, the disk and jet lobes in HH 212 and DG Tau) and between different datasets (*Testi et al.*, 2002; *Woitas et al.*, 2005; *Coffey et al.*, 2005).

Very recently, such findings have been confirmed by the detection of systematic radial velocity shifts in the Near Ultra-Violet (NUV) lines of Mg^+ $\lambda\lambda$ 2796, 2803 (*Coffey et al.*, in preparation). Such lines are believed to arise from the fast, highly excited axial portion of the flow, and can be studied with higher angular resolution. Unfortunately, however, because of the failure of STIS in August 2003, it was only possible to study the jets from Th 28 and DG Tau in the NUV. As expected, the measurements of radial velocity in the NUV lines show slightly higher velocities in the axial region (see Fig. 5). Once again asymmetry in radial velocity across the jet is found. Assuming this is rotation, both the sense of rotation and its amplitude agree with the optical values (see Fig. 5).

Finally, velocity asymmetries compatible with jet rotation have also been detected from the ground using ISAAC on the VLT in two small-scale jets, HH 26 and HH 72, emitting in the H_2 2.12μm line (*Chrysostomou et al.*, 2005). The position-velocity diagrams, again based on slit positions transverse to the outflow, indicate rotation velocities of 5 - 10 $km\,s^{-1}$ at $\approx$ 2-3″ from the source and $\approx$1″ from the jet axis. Note that these jets are driven by Class I sources, suggesting rotation is present, as one would expect, from the earliest epochs.

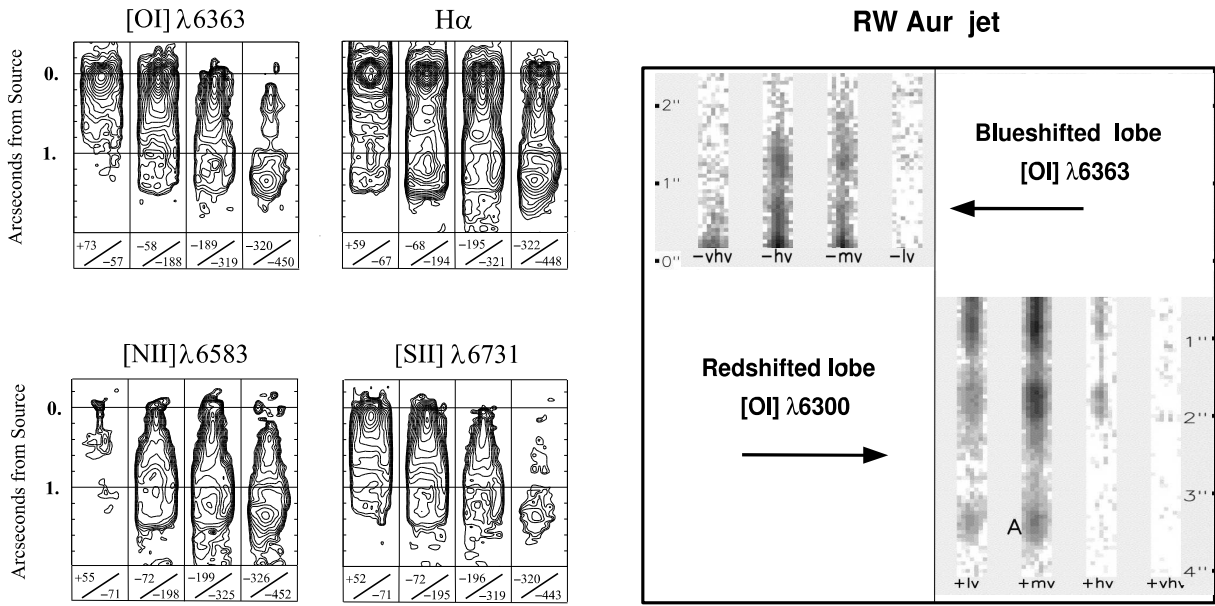The detection of rotation is interesting *per se*, as it sup-

Fig. 3.— 2-D velocity 'channel maps' of the blueshifted jet from DG Tau (left) and of the bipolar jet from RW Aur (right), reconstructed from HST/STIS multi-slit optical spectra. For DG Tau, the low, medium, high and very high velocity intervals are approximately from +60 – -70km s^{-1}(LV), -70 – -195km s^{-1}(MV), -195 – -320km s^{-1}(HV), and -320 – -450km s^{-1}(VHV) respectively. For RW Aur, velocity bins of about 80 km s^{-1} were used starting from -5 km s^{-1}in the approaching lobe and from +11 km s^{-1}in the receding lobe. Note the increase in jet collimation with increasing velocity.
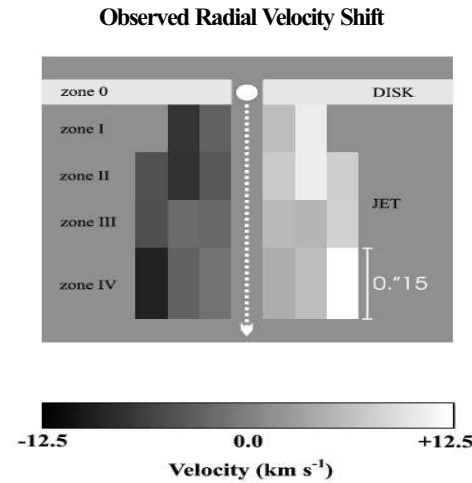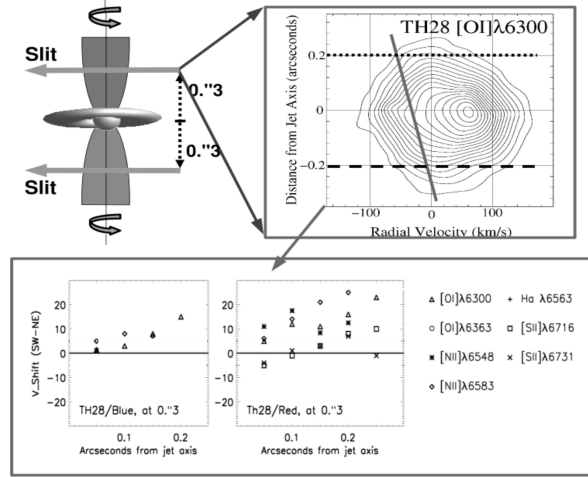

Fig. 4.— Transverse velocity shifts in the optical emission lines detected with HST/STIS across the jets from DG Tau (Left) and Th 28 (Right), at about 50 - 60 AU from the source and 20 - 30 AU from the outflow axis. The application of gaussian fitting and cross-correlation routines to line profiles from diametrically opposite positions centred on the jet axis revealed velocity shifts of 5–25 km s^{-1}. The values obtained suggest toroidal speeds of 10-20 km s^{-1}at the jet boundaries.
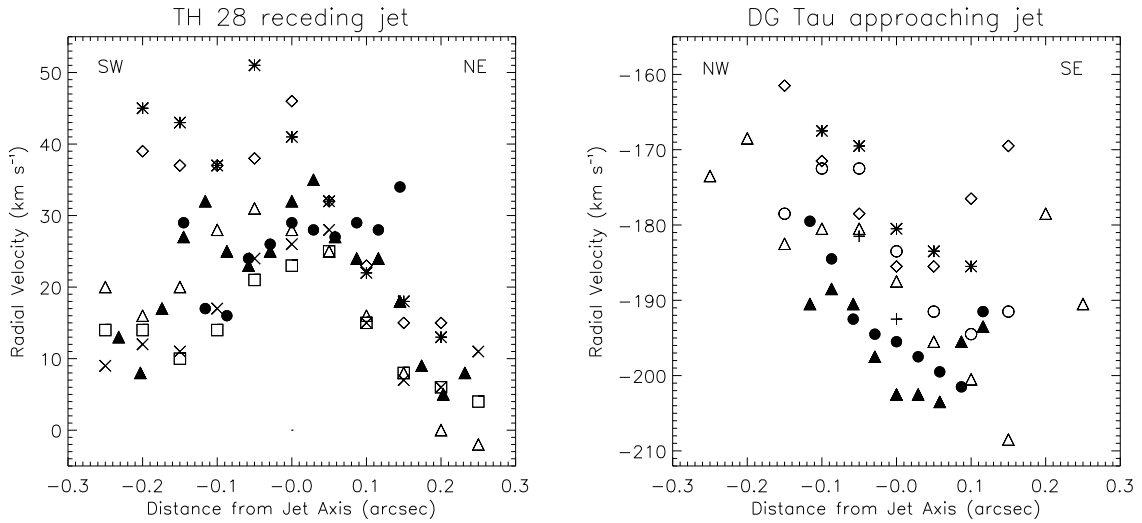
5

Fig. 5.— Radial velocities across the jets from Th 28 (left) and DG Tau (right), in the NUV (solid symbols) and optical (hollow symbols) lines, from HST/STIS spectra taken with the slit transverse to the outflow and at $0\rlap{.}''3$ from the star. The two datasets fit well together. The asymmetry in radial velocity from opposing sides of the jet axis, seen in both wavelength regimes, suggests rotation.

ports the idea that jets are centrifugally launched presumably through the action of a magnetic 'lever-arm'. Assuming that an outflow can be described by a relatively simple steady magneto-hydrodynamic wind model, the application of a few basic equations, in conjunction with the observed velocity shifts, allows us derive a number of interesting quantities that are not yet directly observable. One of these is the *"foot-point radius"*, i.e. the location in the accretion disk from where the observed portion of the jet is launched (*Anderson et al.*, 2003). The observations described here are consistent with foot-point radii between 0.5 and 5 AU from the star, with the NUV (NIR)-emitting layers coming from a location in the disk closer (farther) from the axis than the optical layers. These findings suggest that at least some of the jet derives from an extensive region of the disk (see also *Ferreira et al.*, 2006 who also show intermediate sized magnetic lever arms are favoured). It has to be emphasised however that the current observations only probe the outer streamlines (*Pesenti et al.*, 2004) and accurate determination of the full transverse rotation profile is critical to constrain the models. One cannot, for example, exclude the presence of an inner X-wind at this stage, as the spatial resolution of the measurements is not yet sufficient to probe the axial region of the flow corresponding to any X-wind ejecta (but see *Ferreira et al.*, 2006). Moreover is not absolutely certain that flow lines can be traced back to unique foot-points. In fact, once the region beyond the acceleration zone is reached (typically a few AU above the disk), the wind is likely to undergo various kinds of MHD instabilities that complicate the geometry of the field lines. Thus a one-to-one mapping to a precise foot-point cannot be expected *a priori* (see also below for alternative interpretations of the velocity asymmetries).

Assuming however that the current foot-point determinations are valid, these can be used to get information on the geometry of the magnetic field. In fact from the toroidal and poloidal components of the velocity field one can derive the ratio of the corresponding components of the magnetic field **B**. It is found that at the observed locations $B_\phi/B_p \sim 3-4$ (*Woitas et al.*, 2005). A prevalence of the toroidal field component at 50 - 100 AU from the star is indeed predicted by the models that attribute the collimation of the flow to a magnetic 'hoop stress' (*Königl and Pudritz*, 2000). The most important quantity derived from the observed putative rotation, however, is the amount of angular momentum carried by the jet. In the two systems for which we had sufficient information (namely, DG Tau and RW Aur), we have verified that this is between 60% and 100% of the angular momentum that the inner disk has to loose to accrete at the observed rate. Thus, the fundamental implication of the inferred rotation is that jets are likely to be the major agent for extracting excess angular momentum from the inner disk and in fact this could be their *raison d'être*.

It should be noted how a few recent studies have proposed alternative explanations for the observed velocity asymmetries. For example, they could be produced in asymmetric shocks generated by jet precession (*Cerqueira et al.*, 2006) or by interaction with a warped disk (*Soker*, 2005). It seems unlikely, however, that these alternative models could explain why the phenomenon is so common (virtually all observed jets were found to "rotate") and why the amplitude of the velocity asymmetry is in the range predicted by disk wind theory.

Moreover while the above developments have shed new light on how jets are generated many puzzles remain. For example, a recent study of the disk around RW Aur, sug-

6

gests the disk rotates *in the opposite sense* to both of its jets (*Cabrit et al.*, 2006). Although such observations might be explained by complex interactions with a companion star, it is clear that further studies of jets and disks at high spatial/spectral resolution are needed to definitely confirm the detection of jet rotation.

Another problem is the observed asymmetry in ejection velocity between opposite lobes in a number of outflows. One 'classical' example is the bipolar jet from RW Aur, in which the blueshifted material moves away from the star with a radial velocity $v_{\rm rad} \sim 190$ km s^{-1}, while the redshifted lobe is only moving at ~ 100-110 km s^{-1}. In addition, recent measurements (*López-Martín et al.*, 2003) have shown that the proper motions of the knots in the blue and redshifted lobes are in the same ratio as the radial velocities. This suggests that measured proper motions represent true bulk motions rather than some form of wave. Such findings beg the obvious question: If there are differences in parameters like jet velocity (see also *Hirth et al.*, 1994 for other cases) in bipolar jets, are there differences in even more fundamental quantities such as mass and momentum flux?

What is the origin of the detected near-infrared H$_2$ emission at the base of flows? This apparently comes from layers just external to the jet seen in forbidden lines. Several such 'H$_2$ small-scale jets' have been found recently, as, e.g., HH 72, HH 26, HH 7-11, but H$_2$ winds are also associated with well known jets from T Tauri stars, as, for example, in DG Tau. In the latter case the emission originates from a warm ($T \sim 2000$ K) molecular wind with a flow length and width of 40 and 80 AU, respectively. and has a radial velocity of ~ 15 km s^{-1} (*Takami et al.*, 2004). It is not clear if such a molecular component is entrained by the axial jet, or if it is a slow external component of the same disk wind that generates the fast jet. The latter flow geometry would again agree with model predictions of magneto-centrifugal driven winds.

4. LINE DIAGNOSTICS

The numerous lines emitted by stellar jets, for example from transitions of O^0, S$^+$, N$^+$, Fe$^+$, H, H$_2$, provide a wealth of useful information. By comparing various line ratios and intensities with radiative models, one is able to determine the basic physical characteristics of jets. Not only can we plot the variation of critical parameters such as temperature, ionization, and density in outflows close to their source and in different velocity channels, but also such fundamental quantities as elemental abundances and mass flux rates. Recently spectral diagnostic methods have been extended from the optical into the near infrared. This presents the prospect of not only probing jet conditions in very low velocity shock regions but also gives the opportunity of investigating more embedded jets from less evolved sources. These studies are complementary to the spectral analysis aimed at investigating the disk/star interaction zone and the role of accretion in determining outflow properties.

Determination of the line excitation mechanism in T Tauri stars is a long-standing issue. It is critical in particular for a detailed comparison of wind model predictions with observations. Comparison of the optical line emission properties of the DG Tau and RW Aur jets with what is expected from three different classes of excitation mechanism (mixing layers, ambipolar diffusion, planar shocks) show that line ratios in these jets are best explained by shock excitation with moderate to large velocities (50-100 km s^{-1}) (*Lavalley-Fouquet et al.*, 2000; *Dougados et al.*, 2003) indicating that time variability plays a dominant role in the heating process.

Since Protostars and Planets IV, line diagnostics of stellar jets have developed to the point that not only can we determine the usual quantities such as the electron density (n_e) and temperature (T_e), but a number of additional ones as well. The most important of which is probably *total density*, n_H. In fact all models for the dynamics and radiative properties of jets are highly dependent on this parameter, either directly or through derived quantities such as the jet mass or angular momentum fluxes (see Section 3 and Section 5).
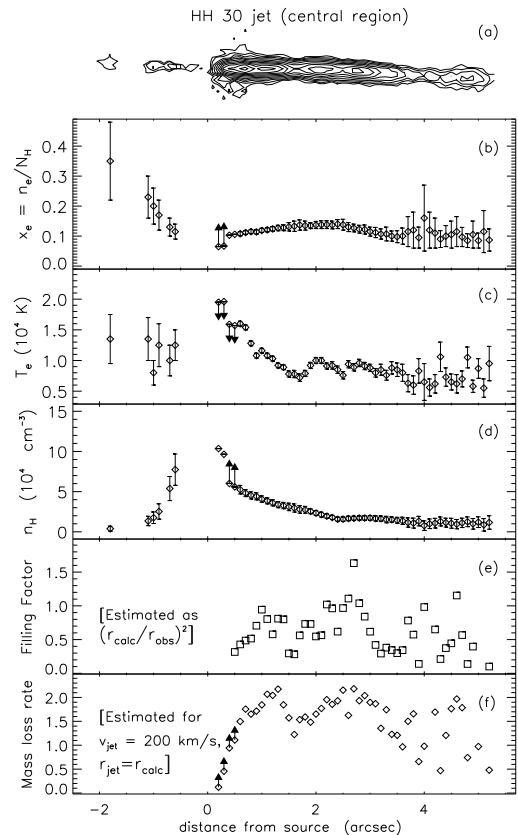

Fig. 6.— Physical quantities along the HH30 jet derived using the BE technique (see text) from HST/WFPC2 narrowband images. From top to bottom: [SII] emission, ionization fraction, electron temperature, total density, filling factor and mass flux in units of 10^{-9} M$_\odot$ yr^{-1} along the jet.

In early studies, as now, physical quantities, such as n_e
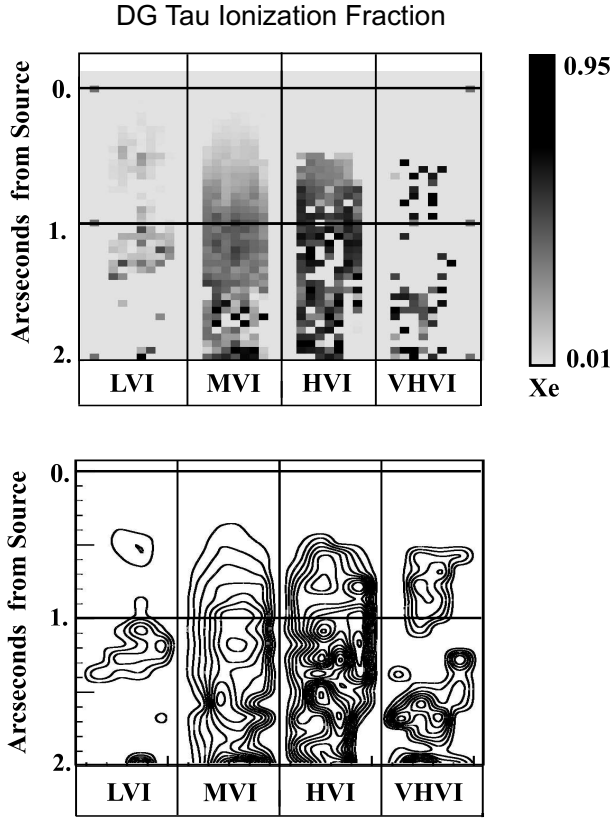
DG Tau Ionization Fraction

Fig. 7.— 2D maps of the level of ionization in the first 200 AU of the DG Tau jet in the different velocity channels indicated in Fig. 3. Ionization values were derived by applying the BE technique to HST/STIS multiple spectra.

and T_e, were determined from line ratios sensitive to these parameters. The observations however were made at low spatial resolution and thus effectively integrated over the shock cooling zone (e.g. *Böhm et al.*, 1980; *Brugel et al.*, 1981). Estimates of other important quantities, such as the ionization fraction and the strength of the pre-shock magnetic field, had to wait for studies in which the observed line intensities and ratios were compared with predicted values based on shock models (e.g., *Hartigan et al.*, 1994). More recently, however, a simpler method, referred to as the 'BE' technique (*Bacciotti and Eislöffel*, 1999) has been developed to measure $x_e = n_e/n_H$ and T_e directly from readily observed optical line ratios utilising transitions of O^0, N^+ and S^+ (*Bacciotti and Eislöffel*, 1999; *Bacciotti*, 2002). The procedure is based on the fact that the gas producing forbidden lines is collisionally excited and no assumptions are made as to the heating mechanism. Such an approach is clearly expedient although not a substitute for a detailed model. The method assumes for example that the emitting gas is at a single temperature, which is not true in the cooling zone behind a shock. That said, one should consider parameters derived from the BE technique as relevant to those regions behind a shock in which the used lines peak in their emission (see the discussion and diagrams in *Bacciotti and*

Eislöffel, 1999).

The basic premise of the BE method is that Sulphur is singly ionised in YSO jets because of its low ionization potential. At the same time the ionization fraction of Oxygen and Nitrogen is assumed to be regulated by charge-exchange with Hydrogen (and recombination). This provides the link between observed line ratios and x_e. The necessary conditions for these assumptions are generally fulfilled in YSO jets. Since however photo-ionization is ignored, applicability of the BE technique is limited to regions far away from any strong sources of UV photons, such at the vicinity of terminal bow-shocks. One must also assume a set of elemental abundances, appropriate for the region under study (see the discussion in *Podio et al.*, in preparation).

A number of jets have been analysed with this technique using moderate resolution long-slit spectra and integral field spectroscopy (*Bacciotti and Eislöffel*, 1999; *Lavalley-Fouquet et al.*, 2000; *Dougados et al.*, 2000; *Nisini et al.*, 2005; *Podio et al.*, in preparation; *Medves et al.*, in preparation). Typical n_e values are found to vary between 50 cm^{-3} and 3.10^3 cm^{-3}, x_e to range from 0.03 to 0.6, and T_e to decrease along a jet from a peak of 2–3 10^4 K close to the source to averages of 1.0–1.4 10^4 K on larger scales. The variation of n_e and x_e along the flow *is consistent with ionization freezing close to the source*, followed by slow non-equilibrium recombination. The mechanism that produces a high degree of ionization close to, although not coincident with, the base of the jet (see Fig. 7), however, is not known. It might, for example, derive from a series of spatially compact non-stationary shocks at the jet base (*Lavalley-Fouquet et al.*, 2000; *Massaglia et al.*, 2005; *Massaglia et al.*, in preparation). Whatever the mechanism a comparison of various jets seems to suggest that it has similar efficiencies in all cases: lower ionization fractions are found in the densest jets, i.e. those that recombine faster. In any event, the realization that stellar jets are only partially ionised has provided new, more accurate estimates of the total density n_H. These estimates are much bigger than previous ones and typically, on large scales, range from 10^3 to 10^5 cm^{-3}. This, in turn, implies that jets can strongly affect their environments, given their markedly increased mass, energy and momentum fluxes. Taking into account typical emissivity filling factors, mass loss rates are found to be about 10^{-8} - 10^{-7} M$_\odot$ yr^{-1} (*Podio et al.*, in preparation) for CTTS jets. The associated linear momentum fluxes (calculated as $\dot{P} = v_{jet}\dot{M}$) are higher, or of the same order, as those measured in associated coaxial molecular flows, where present. This suggests that partially ionised YSO jets could drive the latter.

The BE method is well suited to analysing large datasets, such as those provided by high angular resolution observations. An example of its application, to HST narrow-band images of the HH 30 jet, is shown in Fig. 6 (*Bacciotti et al.*, 1999). A similar analysis of spectra taken from the ground using AO is presented in *Lavalley-Fouquet et al.*, (2000). Even more interesting, is the application of the technique to

the 2-D channel maps reconstructed from parallel slit STIS data (see Fig. 3). In this way one can obtain high angular resolution 2-D maps of the various quantities of interest in the different velocity channels, as illustrated in Fig. 7 for the ionization fraction in the DG Tau jet (*Bacciotti*, 2002; *Bacciotti et al.*, in preparation). The electron density maps, for example, confirm that n_e is highest closest to the star, nearer the axis, and at the highest velocities. At the jet base, one typically finds $0.01 < x_e < 0.4$, and total densities up to 10^6 cm^{-3}. In the same region $8.10^3 < T_e < 2\,10^4$ K. These values can be compared with those predicted by MHD jet launching models. Finally, from n_H, the jet diameter and the de-projected velocity, one can determine the initial mass flux in the jet $\dot{M}_{\rm jet}$. Typical values are found to be around 10^{-7} M$_\odot$ yr^{-1}, with the colder and slower external layers of the jet contributing most to the flux. Such values can be combined with known accretion rates in these stars to produce $\dot{M}_{\rm jet}/\dot{M}_{\rm acc}$ ratios. Note that accretion rates are determined independently through line veiling (*Hartigan et al.*, 1995). Typical ratios in the range $0.05 - 0.1$ are found. This seems inconsistent with cold disk wind models although warm disk winds with moderate magnetic lever arms are expected to produce such ratios (*Casse and Ferreira*, 2000).

In the last few years application of line diagnostics has been extended from the optical into the near infrared (*Nisini et al.*, 2002; *Pesenti et al.*, 2003; *Giannini et al.* 2004; *Hartigan et al.*, 2004). As stated at the beginning of this section, this presents the prospect of not only probing jet conditions in very low velocity shock regions but also the possibility of investigating more embedded, and less evolved jets. For example, using NIR lines of Fe$^+$, one can determine not only the electron density in denser embedded regions of the jet, but also such fundamental quantities as the visual extinction A$_V$ along the line of sight to an outflow. Note that A$_V$ has to be known if we are to correct line ratios using lines that are far apart in wavelength. In addition, the NIR H$_2$ lines provide a probe of excitation conditions in low velocity shocks near the base of the flow where some molecular species survive.

Very recently, the potential of a combined optical/NIR set of line diagnostics has been exploited (*Nisini et al.*, 2005; *Podio et al.*, in preparation), using a variety of transitions in the 0.6 to 2.2 μm range. This approach has turned out to be a very useful means of determining how physical quantities vary in the different stratified layers behind a shock front as well as providing additional checks on many parameters. For example, the combination of red and NIR Fe$^+$ lines gives an independent estimate of T$_e$ and n$_e$, which does not rely on the choice of elemental abundances. The electron density and temperature, derived from Iron lines, turn out to be higher and lower respectively, than those determined from optical lines. This is in agreement with the prediction that Iron emission should, on average, come from a region within the post-shock cooling zone that is farther from the shock front than those regions giving rise to the optical lines. Hence it is cooler and of higher density.

Moreover analysis of NIR Ca$^+$ and C^0 lines show that jets possess regions of even higher density (n$_H$ up to 10^6 cm^{-3}). Finally, various lines have been used to estimate the depletion onto dust grains of Calcium and Iron with respect to solar values. The amount of depletion turns out to be quite substantial: around 30-70% for Ca and 90% for Iron. This leads to the suggestion that the weak shocks present in many jets are not capable of completely destroying ambient dust grains, as expected theoretically (*Draine*, 1995).

5. PROBING THE OUTFLOW ON AU SCALES: USE OF SPECTRO-ASTROMETRY

As this review (and others in this volume) shows, there has been a dramatic improvement over the past decade in the spatial information provided by modern instrumentation, with arguably the most detail delivered by the HST (e.g., *Bacciotti et al.*, 2000). AO also played an important role in allowing us to peek closer to the YSO itself (e.g., *Dougados et al.*, 2002). Nevertheless, it still remains true that the spatial resolution of astronomical observations are constrained by the diffraction limit of the telescope (as well as optical aberrations and atmospheric seeing in many cases). In order to probe down to the central engine, we need to achieve a resolution of ~ 10 AU or better which corresponds to $\lesssim 0.05''$ for the nearest star forming regions. In other words, we need milliarcsecond resolution!

Here we briefly describe the technique of spectro-astrometry and how it can be used to determine the spatio-kinematic structure of sources well below the diffraction limit of the telescope, and then review some of the important results obtained using this technique.

The great value and appeal of spectro-astrometry lies in its rather simple application and the fact that it does not require specialist equipment nor the best weather conditions. With no more than a standard CCD in a long-slit spectrograph, we have in return a tool which is capable of probing emission structures within AU scales of the YSO. An unresolved star is observed with a long-slit spectrograph and the positional centroid of the emission along the slit is determined as a function of wavelength. If the unresolved source consists of an outflow or binary with distinctive features in their spectra, the centroid position will shift relative to the continuum at the wavelength of the features. As such, the only factor which affects the accuracy of this technique is the ability to measure an accurate centroid position and this is ultimately governed by the number of photons detected and a well sampled seeing profile (hence a small pixel scale, with the added requirement of a uniform CCD). Each photon detected should be within a distance, defined by the seeing disk, from the centroid and the uncertainty in this position reduces by $\sqrt{N}$ when N photons are detected. This results in a position spectrum whose accuracy, measured in milliarcseconds, is given by $\Delta x \sim 0.5 \times {\rm FWHM}_{\rm seeing}/\sqrt{N}$ (*Takami et al.*, 2003). Consequently, brighter emission lines are better suited to probing the inner regions of the YSO.

As *Bailey*, (1998) explains, the method is not new and has been used in previous works, although these involved specialist techniques and equipment (*Beckers*, 1982; *Christy, Wellnitz and Currie*, 1983). Moreover a number of authors (e.g., *Solf and Böhm*, 1993 and *Hirth et al.*, 1997) have used long-slit spectroscopy to examine sub-arcsecond kinematic structure of the HVC and LVC in a number of outflows. *Bailey*, (1998) revived interest in the technique by demonstrating that one could routinely recover information on milliarcsecond scales by taking long-slit spectra at orthogonal and anti-parallel position angles, i.e. by rotating the instrument and pairing spectra taken at $0°$ & $180°$ and $90°$ & $270°$ apart. Each anti-parallel pair is subtracted to remove any systematic errors introduced by the telescope and/or instrument, as such signals should be independent of rotation whereas the true astronomical signal is reversed (see also *Brannigan et al.*, in preparation).

5.1. Spectro-astrometry – the science

The first extensive use of spectro-astrometry came with the study of *Bailey*, (1998) who used it to prove the technique on known binaries, in the course of which two previously unknown binaries were also discovered. Since then, *Garcia et al.*, (1999) and *Takami et al.*, (2001, 2003) have surveyed a number of YSOs revealing jets on scales of ~ 10 AU from the source in a few cases. Perhaps most interesting, are discoveries of *bipolar* jets at these small scales.

Forbidden lines only trace outflows in those zones with less than the critical electron density for the line. As jets tend to have higher densities closer to their source, this means that a point is reached where individual forbidden lines fade. In contrast, a permitted line traces activity all the way to the star. Such lines, e.g. Hα, however not only map outflows but magneto-spheric accretion onto the YSO as well (e.g., *Muzerolle et al.*, 1998). It follows that the profile of a permitted line at the star tends to be a mixture of outflow and inflow components. As we will show, spectro-astrometry is a way of unravelling these respective contributions. Now as mentioned previously, if a spectrum is taken of a CTTS, it tends only to show blueshifted forbidden lines. This is readily understandable if the forbidden line emission comes only from an outflow and the redshifted (counter-flow) at the star is obscured by an accretion disk (a view that is also endorsed by spectro-astrometry). Now if we search for a spectro-astrometric offset in the blue-shifted wing of a permitted line we find the maximum offset at the blueshifted jet velocity and in the same direction. The offsets however are much smaller than those measured for the forbidden lines, implying the permitted emission tends to come from much closer to the source. Remarkably *Takami et al.*, (2001, 2003) found bipolar Hα emission centred on RU Lupi and CS Cha, clearly indicating a direct line of sight to the counter-flow through the accretion disk in these stars. This is interpreted as evidence of a sizable gap or dust hole in the disk at a radius of $\sim 1 - 5$ AU from the protostar. The gap itself could be generated by a planetary body (see,

for example, *Varniére et al.*, 2005) although it could equally be due to the development of very large dust grains in the innermost region of the disk (see, for example, *Watson and Stapelfeldt*, 2004). Such large dust grains would have reduced opacity. Supporting evidence for the presence of gaps is seen in the spectral energy distributions of these objects; they show mid-infrared emission dips consistent with temperatures of ~ 200 K, coincident with the ice condensation temperature where the increase in surface density may aid planet formation (*Boss*, 1995).

Recently the technique has been used in the near-infrared. As well as allowing us to investigate younger and more embedded sources, this wavelength range also makes available other lines as probes. For example, Paβ (1.2822 μm) is found in the spectra of many T-Tauri stars and was believed to exclusively trace accretion. *Whelan et al.*, (2004) showed however that this is not always the case using spectro-astrometry. In particular large spatial offsets relative to the YSO were found in the line wings (something which would not be expected in the case of accretion). Magneto-spheric accretion models have always struggled to explain the detailed profiles of permitted lines (*Folha and Emerson*, 2001). Spectro-astrometry seems to have resolved this problem by identifying those parts of the line attributable to an outflowing jet. It is also worth noting that both *Takami et al.*, (2001) and *Whelan et al.*, (2004) show evidence which suggests that offsets from the star increases with velocity, consistent with the presence of an acceleration zone.

Finally, *Whelan et al.*, (2005) used spectro-astrometry to report the first detection of an outflow from a brown dwarf. Their data suggest many similarities (allowing for scaling factors) between the brown dwarf outflow and those seen in CTTS. Observations, such as these, suggest a universal correlation between the gravitational collapse of an object with an accretion disk and the generation of an outflow.

6. FROM BROWN DWARFS to HERBIG Ae/Be STARS

It is conceivable that the accretion/ejection mechanism responsible for the generation and collimation of jets becomes substantially modified, or may not even operate, as one goes to sources of substantially higher or lower mass than T Tauri stars. Thus, it is an interesting question if such objects also produce jets and if they are similar to those from CTTS. Certainly exploring how outflows vary with the mass of the central object (varying escape velocity, radiation field, etc) can provide useful constraints and tests for any proposed accretion/ejection model.

Recent studies have detected signatures of accretion in a wide range of objects from brown dwarfs, with masses as low as 0.03 M$_\odot$ (*Jayawardhana et al.*, 2003; *Natta et al.*, 2004; *Mohanty et al.*, 2005), through Very Low Mass (VLM) stars (*Scholz and Eislöffel*, 2004) to Herbig Ae/Be stars (*Finkenzeller*, 1985; *Böhm and Catala*, 1994; *Corcoran and Ray*, 1997) of 2-10 M$_\odot$. While the accretion rates
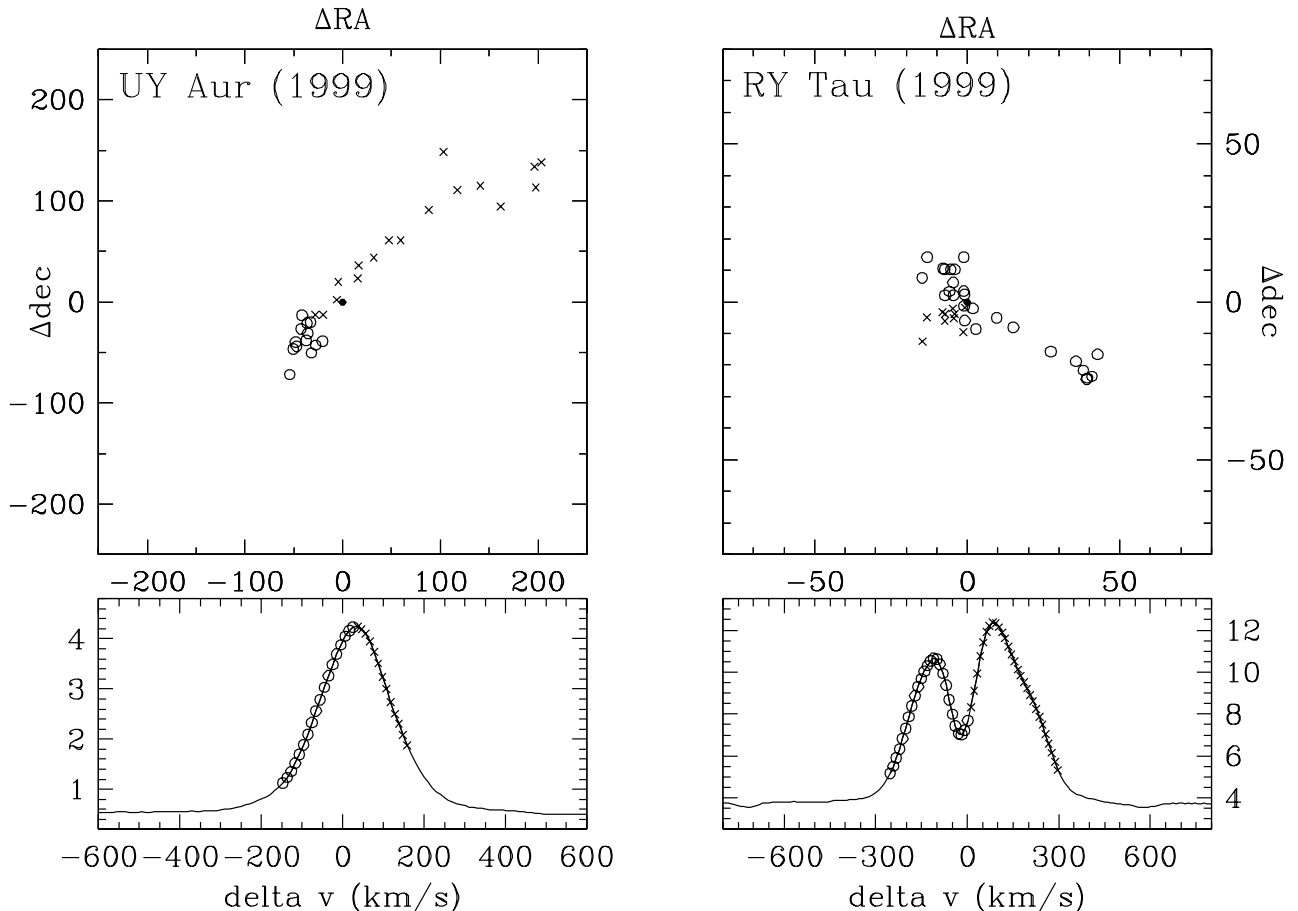
Fig. 8.— Example spectro-astrometry data of the Hα line. The upper panels show x-y plots of the spectro-astrometric offsets at each position across the line profile (circles and crosses for blue- and red-shifted components, respectively). The integrated line profile is shown below. The data were taken using the ISIS instrument on the William Herschel Telescope on La Palma. *Left*: Detection of a *bipolar* outflow in UY Aur implying the presence of a disk gap in this object. *Right*: The same for RY Tau although the evidence suggests either a binary companion or a mono-polar jet with the red-shifted component hidden from view.

show a large spread at any given mass, it seems that a relationship $\dot{M}_{acc} \propto M_{obj}^2$ holds for the upper envelope of the distribution (see, for example, *Natta et al.*, 2004). This dependence is much steeper than expected from viscous disk models with a constant viscosity parameter α, which would predict a much shallower relationship (*Natta et al.*, 2004; *Mohanty et al.*, 2005). Strongly varying disk ionisation with the central object mass caused by its X-ray emission (*Muzerolle et al.*, 2003) or disk accretion controlled by Bondi-Hoyle accretion from the large gas reservoir of the surrounding cloud core (*Padoan et al.*, 2005) have been proposed to understand the steep relationship between accretion rate and central object mass.

In order to estimate the minimum mass of a source that we might be able to detect an outflow from, it is plausible to extrapolate the known linear correlation between ejection and accretion rates. Moreover *Masciadri and Raga*, (2004) have shown that the luminosity of a putative brown dwarf jet should scale approximately with its mass outflow rate.

Thus, giving the known accretion rates of brown dwarfs, we expect their outflows to be about 100 times fainter at best than those from CTTS, i.e. just within the reach of the biggest telescopes (*Whelan et al.*, 2005).

The first very low mass object, LS-RCrA-1 found to show forbidden lines typical of outflows from T Tauri stars, was discovered by *Fernández and Comerón*, (2001). Its mass has been estimated as substellar (*Barrado y Navascués et al.*, 2004), but the forbidden line emission could not be resolved spatially (*Fernández and Comerón*, 2005). In the same work, however, a 4″-long jet and a 2″-long counterjet were reported on from the VLM star Par-Lup3-4. Simultaneously *Whelan et al.*, (2005) detected a spatially resolved outflow from the 60 Jupiter-mass brown dwarf ρ Oph 102, using spectro-astrometry. The outflow is blue-shifted, by about -50 km s^{-1} with respect to its source, and has characteristics similar to those from CTTS.

Moving to the other end of the mass spectrum, it is also interesting to investigate if the intermediate mass Herbig

Ae/Be stars show accretion/ejection structures like those of the lower mass T Tauri stars. Several large-scale Herbig-Haro flows have been known for some time, which may be driven by Herbig Ae/Be stars. In many cases however it is not certain that the Herbig Ae/Be star, as opposed to a nearby, unrelated T Tauri star or a lower mass companion, could be responsible. Examples include HH39 associated with R Mon (*Herbig*, 1968), HH218 associated with V645 Cyg (*Goodrich*, 1986), and HH215 and HH315 associated with PV Cep (*Neckel et al.*, 1987; *Gomez et al.*, 1997; *Reipurth et al.*, 1997). The first jet that could unambiguously be traced back to a Herbig Ae/Be star was HH398 emanating from LkHα 233 (*Corcoran and Ray*, 1998). All these outflow sources exhibit blue-shifted forbidden emission lines in their optical spectra with typical velocities of a few hundred km s^{-1}, similar to CTTS.

More recently, small-scale jets from two nearby Herbig Ae stars have been found by coronographic imaging in the ultraviolet with the HST. These jets and counterjets from HD163296 (HH409, *Devine et al.*, 2000; *Grady et al.*, 2000) and HD104237 (HH669, *Grady et al.*, 2004) are only a few arcseconds long. They are readily seen in Lyα as the contrast between the star and the shocked flow is much more favourable than in the optical: Lyα/H$\alpha \geq 10$ according to shock models (e.g. *Hartigan et al.*, 1987).

Summarising, we find that Herbig-Haro jets both in the form of small-scale jets and parsec-scale flows are ubiquitous in CTTS. They seem to be much rarer towards the higher mass Herbig AeBe stars, and only one clear example of an outflow from a brown dwarf is known so far. Nevertheless this seems to indicate that the accretion/ejection structures in all objects are similar and the same physical processes are at work over the whole mass spectrum. The conditions for the generation of jets seem to be optimal in CTTS T Tauri stars, while under the more extreme environments, both in the lower mass brown dwarfs and in the higher mass Herbig Ae/Be stars, jet production could be less efficient. Current models of the magneto-centrifugal launching of jets from young stars will have to be tested for the conditions found in brown dwarfs and Herbig AeBe stars, in order to see if they are can reproduce the frequency and physical characteristics of the observed flows.

7. THE FUTURE: TOWARDS RESOLVING THE CENTRAL AU

While it is clear from this review that high angular resolution observations (on scales $\approx 0''.1$) have provided important information on the launch mechanism, the true 'core' of the engine lies below the so-called 'Alfvèn surface'. This surface is located within a few AU of the disk (i.e. tens of milliarcseconds for the nearest star forming region) so the core cannot be resolved with conventional instrumentation either from the ground or space. This, however, is about to change with the new generation of optical/NIR interferometers coming on-stream, opening up the exciting possibility of exploring this region for the first time. Two facilities

are being rolled out at present in which Europe will play an active role: the VLT Interferometer (VLTI) at ESO-Paranal, and the Large Binocular Telescope (LBT) at Mount Graham in Arizona.

The VLTI will operate by connecting, in various combinations, up to four 8-m and four smaller (1.8-m) auxiliary telescopes. The latter can move on tracks to a number of fixed stations so as to obtain good *(u,v)* plane coverage. The beams, of course, from the various telescopes have to be combined in a correlator. In this regard the AMBER instrument is of particular interest to the study of YSO jet sources as it allows for medium resolution spectroscopy in the NIR (e.g. high velocity Paschen β emission). AMBER, can combine up three AO corrected beams, thus allowing "closure phase" to be achieved and it will provide angular resolution as small as a few milliarcseconds. In the early days of operating this instrument, incomplete *(u,v)* plane coverage is expected and in this case models of the expected emission are needed to interpret the observations (*Bacciotti et al.*, 2003). The LBT Interferometer, in contrast to the VLTI, is formed by combining the beams of two fixed 8.4-m telescopes and hence has a fixed baseline. Effectively it will have the diffraction limited resolution of a 23-m telescope (*Herbst*, 2003) and excellent *(u,v)* plane coverage because of the shortness of the baseline in comparison to the telescope apertures. Moreover it will complement the VLTI through its short projected baseline spacings, spacings that are inaccessible to the former. The LBT Interferometer will initially operate in the NIR in so-called Fizeau mode providing high resolution images over a relatively large field of view (unlike the VLTI). A future extension into the optical is however planned.

Radio provides a means of obtaining high spatial resolution observations of YSO jets close to their source if the source is highly embedded (*Girart et al.*, 2002). Their free-free emission, however, tends to be rather weak and so the number of outflows mapped so far at radio wavelengths has been quite small. This will change dramatically when the new generation of radio interferometers, in particular e-MERLIN (extended MERLIN) and EVLA (extended VLA), come on-line. Although there will be modest improvements in resolution, the primary gain will be in sensitivity allowing, in some cases, the detection of emission 20-50 weaker than current thresholds. This increase in sensitivity will be achieved through correlators and telescope links with much broader band capacities than before. Such improvements will not only lead to the detection of more jet sources, and hopefully allow meaningful statistical studies, but perhaps more importantly to the detection of non-thermal components in known outflows as already hinted at in a number of studies (see *Girart et al.*, 2002; *Ray et al.*, 1997; *Reid et al.*, 1995). Polarization studies of such emission in turn would give us a measure of ambient magnetic field strength and direction, parameters that are poorly known at present. Finally it is worth noting that a number of studies have shown that H$_2$O masers may in some instances be tracing outflows (*Claussen et al.*, 1998; *Torrelles et al.*,

2005) and not circumstellar disks as often assumed. High resolution polarization studies of such masers can not only provide information on magnetic field strengths and direction but, when combined with multi-epoch studies, information on how the magnetic fields evolve with time (*Baudry and Diamond*, 1998).

The other large interferometric facility being planned for observations at the sub-mm wavelength range is ALMA, an array of 64 12m antennas to be built in the Atacama desert in Chile, not far from the VLTI site. With ALMA we will be able not only to routinely measure disk rotation but also conceiveably rotation in molecular outflows if present. The future therefore for this field is very bright indeed.

REFERENCES

Anderson, J. M., Li, Z.-Y., Krasnopolsky, R., and Blandford, R. (2003) *Astrophys. J., 590*, L107-L110.

Bacciotti, F. (2002) *Rev. Mex. Astron. Astrofis., 13*, 8-15.

Bacciotti, F. and Eislöffel, J. (1999) *Astron. Astrophys., 342*, 717-735.

Bacciotti, F., Eislöffel, J., and Ray, T.P. (1999) *Astron. Astrophys., 350*, 917-927.

Bacciotti, F., Mundt, R., Ray, T.P., Eislöffel, J., Solf, J., and Camenzind, M. (2000) *Astrophys. J., 537*, L49-L52.

Bacciotti, F., Ray, T.P., Mundt, R., Eislöffel, J., and Solf, J. (2002) *Astrophys. J., 576*, 222-231.

Bacciotti, F., Testi, L., Marconi, A., Garcia, P. J. V., Ray, T. P., Eislöffel, J., and Dougados, C. (2003) *Astrophys. Sp. Sci., 286*, 157-162.

Bailey, J.A. (1998) *Mon. Not. Roy. Astr. Soc., 301*, 161-167.

Barrado y Navascués, D., Mohanty, S., and Jayawardhana, R. (2004) *Astroph. J., 604*, 284-296.

Baudry, A. and Diamond, P. J. (1998) *Astron. Astrophys., 331*, 697-708.

Beckers, J. (1982) *Opt. Acta, 29*, 361-362.

Böhm, T. and Catala, C. (1994) *Astron. Astrophys., 290*, 167-175.

Böhm, K. H., Mannery, E., and Brugel, E. W. (1980) *Astrophys. J., 235*, L137-L141.

Boss, A. (1995) *Science, 267*, 360-362.

Brugel, E. W., Böhm, K. H., and Mannery, E. (1981) *Astrophys. J. Suppl., 47*, 117-138.

Cabrit, S., Edwards, S., Strom, S. E., and Strom, K. M. 1990, *Astrophys. J., 354*, 687-700

Cabrit, S., Pety, J., Pesenti, N., and Dougados, C. (2006) *Astron. Astrophys.*, in press.

Casse, F., and Ferreira, J. 2000, *Astron. Astrophys., 353*, 1115-1128

Cerqueira, A. H., Velazquez, P. F., Raga, A. C., Vasconcelos, M. J., and De Colle, F. (2006) *Astron. Astrophys.*, in press.

Christy, J., Wellnitz, D., and Currie, D. (1983) In *Current Techniques in Double and Multiple Star Research* R. Harrington and O. Franz, eds.) (IAU Coll. 62), *Lowell Obs. Bull., 167*, 28-35.

Chrysostomou, A., Bacciotti, F., Nisini, B., Ray, T. P., Eislöffel, J., Davis, C. J., and Takami, M. (2005) In *PPV Poster Proceedings* http://www.lpi.usra.edu/meetings/ppv2005/pdf/8156.pdf

Claussen, M. J., Marvel, K. B., Wootten, A., and Wilking, B. A. (1998) *Astrophys. J.*, 507, L79-L82.

Corcoran, M. and Ray, T. P. (1997) *Astron. Astrophys., 321*, 189-201.

Corcoran, M. and Ray, T. P. (1998) *Astron. Astrophys., 336*, 535-538.

Coffey, D., Bacciotti, F., Ray, T. P., Woitas, J., and Eislöffel, J. (2004) *Astrophys. J., 604*, 758-765.

Coffey, D. A., Bacciotti, F., Woitas, J., Ray, T. P., and Eislöffel, J. (2005) In *PPV Poster Proceedings* http://www.lpi.usra.edu/meetings/ppv2005/pdf/8032.pdf

Davis, C. J., Berndsen, A., Smith, M. D., Chrysostomou, A., and Hobson, J. (2000) *Mon. Not. Roy. Astr. Soc., 314*, 241-255.

Draine, B. T. (1995) *Astrophys Space Sci., 233*, 111-123.

Devine, D., Grady, C.A., Kimble, R.A., Woodgate, B., Bruhweiler, F.C., Boggess, A., Linsky, J.L., and Clampin, M. (2000) *Astroph. J., 542*, L115-L118.

Dougados, C., Cabrit, S., Ferreira, J., Pesenti, N., Garcia, P., and O'Brien, D. (2004) *Astrophys Space Sci., 292*, 643-650.

Dougados, C., Cabrit, S., Lavalley, C., and Ménard, F. (2000) *Astron. Astrophys., 357*, L61-L64.

Dougados, C., Cabrit, S., and Lavalley-Fouquet, C. (2002) *Rev. Mex. Astron. Astrofis., 13*, 43-48.

Dougados, C., Cabrit, S., Lopez-Martin, L., Garcia, P., and O'Brien, D. (2003), *Astrophys. Space Sci., 287*, 135-138

Dougados, C., Cabrit, S., Ferreira, J., Pesenti, N., Garcia, P., and O'Brien, D. (2004) *Astrophys. Space Sci., 293*, 45-52

Eislöffel, J., Mundt, R., Ray, T. P., and Rodríguez, L. F. (2000) In *Protostars and Planets IV* (V. Mannings et al., eds.), pp. 815-840. Univ. of Arizona, Tucson.

Fernández, M. and Comerón, F. (2001) *Astron. Astrophys., 380*, 264-276.

Fernández, M., and Comerón, F. (2005) *Astron. Astrophys., 440*, 1119-1126.

Ferreira, J. (1997) *Astron. Astrophys., 319*, 340-359.

Ferreira, J., Dougados, C., and Cabrit, S. (2006) *Astron. Astrophys.*, in press.

Finkenzeller, U. (1985) *Astron. Astrophys., 151*, 340-348.

Folha, D. F. M. and Emerson, J. P. (2001) *Astron. Astrophys.*, 365, 90-109.

Frank, A., and Mellema, G. (1996) *Astrophys. J., 472*, 684-702.

Garcia, P. J. V., Thiébaut, E., and Bacon, R. (1999) *Astron. Astrophys., 346*, 892-896.

Garcia, P.J.V., Cabrit, S., Ferreira, J., and Binette, L. (2001), *Astron. Astrophys., 377*, 609-616.

Girart, J. M., Curiel, S., Rodríguez, L. F., and Cantó, J. 2002, *Rev. Mex. Astron. Astrofis., 38*, 169-186.

Giannini, T., McCoey, C., Caratti o Garatti, A., Nisini, B., Lorenzetti, D., and Flower, D. R., (2004) *Astron. Astrophys., 419*, 999-1014.

Goodson, A. P., Böhm, K.-H., and Winglee, R. M. (1999) *Astroph. J., 524*, 142-158.

Gomez, M., Kenyon, S.J., and Whitney, B.A. (1997) *Astron. J., 114*, 265-271.

Goodrich, R. (1986) *Astroph. J., 311*, 882-894.

Grady, C.A., Devine, D., Woodgate, B., Kimble, R., Bruhweiler, F.C., Boggess, A., Linsky, J.L., Plait, P., Clampin, M., and Kalas, P. (2000) *Astroph. J., 544* 895-902.

Grady, C.A., Woodgate, B., Torres, C.A.O., Henning, T., Apai, D., Rodmann, J., Wang, H., Stecklum, B., Linz, H., Willinger, G.M., Brown, A., Wilkinson, E., Harper, G.M., Herczeg, G.J., Danks, A., Vieira, G.L., Malumuth, E., Collins, N.R., and Hill, R.S. (2004) *Astroph. J., 608*, 809-830.

Hartigan, P., Edwards, S., and Gandhour, L. (1995) *Astrophys. J., 452*, 736-768.

Hartigan, P., Edwards, S., and Pierson, R. (2004) *Astrophys. J., 609*, 261-276.

Hartigan, P., Morse, J., and Raymond, J. (1994) *Astroph. J., 436*, 125-143.

Hartigan, P., Raymond, J., and Hartmann, L. (1987) *Astroph. J., 316*, 323-348.

Herbig, G. (1968) *Astroph. J., 152*, 439-441.

Herbst, T. (2003) *Astrophy. Sp. Sci., 286*, 45-53.

Hirth, G. A., Mundt, R., and Solf, J. (1997) *Astron. Astrophys. Suppl., 126*, 437-469.

Hirth, G. A., Mundt, R., Solf, J., and Ray, T. P. (1994) *Astroph. J., 427*, L99-L102.

Jayawardhana, R., Mohanty, S., and Basri, G. (2003) *Astroph. J., 592*, 282-287.

Königl, A. and Pudritz, R. (2000) In *Protostars and Planets IV* (V. Mannings et al., eds.), pp. 759-788. Univ. of Arizona, Tucson.

Lavalley, C., Cabrit, S., Dougados, C., Ferruit, P., and Bacon, R. (1997) *Astron. Astrophys., 327*, 671-680.

Lavalley-Fouquet, C. Cabrit, S. and Dougados, C. (2000) *Astron. Astrophys., 356*, L41-L44.

Livio, M. (2004) *Baltic Astronomy, 13*, 273-279.

López-Martín, L., Cabrit, S., and Dougados, C. (2003) *Astron. Astrophys., 405*, L1-L4.

Masciadri, E. and Raga, A.C. (2004) *Astroph. J., 615*, 850-854.

Massaglia, S., Mignone, A., Bodo, G., (2005) *Astron. Astrophys., 442*, 549-554

Massaglia, S., Mignone, A., Bodo, G., Bacciotti, F. (2006) *Astron. Astrophys.*, in press.

McGroarty, F. and Ray, T. P. (2004), *Astron. Astrophys., 420*, 975-986.

Mohanty, S., Jayawardhana, R., and Basri, G. (2005) *Astroph. J., 626*, 498-522.

Mundt, R. and Eislöffel, J. (1998) *Astron. J., 116*, 860-867.

Muzerolle, J., Calvet, N., and Hartmann, L. (1998) *Astroph. J., 492*, 743-753.

Muzerolle, J., Hillenbrand, L., Calvet, N., Briceño, C., and Hartmann, L. (2003) *Astroph. J., 592*, 266-281.

Natta, A., Testi, L., Muzerolle, J., Randich, S., Comerón, F., and Persi, P. (2004) *Astron. Astrophys., 424*, 603-612.

Neckel, T., Staude, H.J., Sarcander, M., and Birkle, K. *Astron. Astrophys., 175*, 231-237.

Nisini, B., Bacciotti, F., Giannini, T., Massi F., Eislöffel, J., Podio, L., and Ray, T.P. (2005) *Astron. Astrophys., 441*, 159-170.

Nisini, B., Caratti o Garatti, A., Giannini, T., and Lorenzetti, D. (2002) *Astron. Astrophys., 393*, 1035-1051.

Padoan, P., Kritsuk, A., Norman, M., and Nordlund, A. (2005) *Astroph. J., 622*, L61-L64.

Pesenti, N., Dougados, C., Cabrit, S., O'Brien, D., Garcia, P., and Ferreira, J. (2003) *Astron. Astrophys., 410*, 155-164.

Pesenti, N., Dougados C., Cabrit S., Ferreira J., O'Brien D., and Garcia P. (2004) *Astron. Astrophys., 416*, L9-L12.

Pyo, T.-S., et al. 2003, *Astrophy. Space Sci., 287*, 21-24.

Raga, A., Cabrit, S., Dougados, C., and Lavalley, C. (2001) *Astron. Astrophys., 367*, 959-966

Ray, T. P., Mundt, R., Dyson, J. E., Falle, S. A. E. G., and Raga, A. C. (1996) *Astrophys. J., 468*, L103-L106.

Ray, T. P., Muxlow, T. W. B., Axon, D. J., Brown, A., Corcoran, D., Dyson, J., and Mundt, R. (1997) *Nature, 385*, 415-417.

Reid, M. J., Argon, A. L., Masson, C. R., Menten, K. M., and Moran, J. M. (1995) *Astrophys. J., 443*, 238-244.

Reipurth, B. and Bally, J. (2001) *Ann. Rev. Astron. Astrophys., 39*, 403-455.

Reipurth, B., Bally, J., and Devine, D. (1997) *Astron. J., 114*, 2708-2735.

Scholz, A. and Eislöffel, J. (2004) *Astron. Astrophys., 419*, 249-267.

Shang, H., Glassgold, A.E., Shu, F.H., and Lizano, S. (2002) *Astrophys. J., 564*, 853-876.

Shu, F. H., Najita, J. R., Shang, H., and Li, Z.-Y. (2000) In *Protostars and Planets IV* (V. Mannings et al., eds.), pp. 789-814. Univ. of Arizona, Tucson.

Soker, N., (2005) *Astron. Astrophys., 435*, 125-129.

Solf, J. and Böhm, K.H. (1993) *Astroph. J., 410*, L31-L34.

Takami, M., Bailey, J.A., and Chrysostomou, A. (2003) *Astron. Astrophys., 397*, 675-691.

Takami, M., Bailey, J.A., Gledhill, T.M., Chrysostomou, A., and Hough, J.H. (2001) *Mon. Not. Roy. Astr. Soc., 323*, 177-187.

Takami, M., Chrysostomou, A., Ray, T. P., Davis, C., Dent, W. R. F., Bailey, J., Tamura, M., and Terada, H. (2004) *Astron. Astrophys., 416*, 213-219.

Testi, L., Bacciotti, F., Sargent, A. I., Ray, T. P., and Eislöffel, J. (2002), *Astron. Astrophys., 394*, L31-L34.

Torrelles, J. M., Patel, N., Gómez, J. F., Anglada, G., and Uscanga, L. (2005), *Astrophys. Space Sci., 295*, 53-63.

Varniére, P., Blackman, E.C, Frank, A., and Quillen, A.C. (2005) In *PPV Poster Proceedings* http://www.lpi.usra.edu/meetings/ppv2005/pdf/8064.pdf

Watson, A. M., and Stapelfeldt, K. R. (2004) *Astrophys. J., 602*, 860-874.

Whelan, E., Ray, T.P., and Davis, C.J. (2004) *Astron. Astrophys., 417*, 247-261.

Whelan, E.T., Ray, T.P., Bacciotti, F., Natta, A., Testi, L., and Randich, S. (2005) *Nature, 435*, 652-654.

Woitas, J., Ray, T.P., Bacciotti, F., Davis, C.J., and Eislöffel, J. (2002) *Astrophys. J., 580*, 336-342.

Woitas, J., Bacciotti, F., Ray, T.P., Marconi, A., Coffey, D., and Eislöffel, J., (2005) *Astron. Astrophys., 432*, 149-160.